

Effect of Drag-Reducing Polymers on Mass Transfer Fluctuations

Electrochemical techniques are used to show that drag-reducing polymers decrease the magnitude and the frequency of mass transfer fluctuations. Measurements of the frequency spectrum of the mass transfer fluctuations allow calculation of the normal component of velocity fluctuations in the immediate vicinity of the wall. This information is used to interpret the observed effect of drag-reducing polymers on the rate of mass transfer.

Eleni Vassiliadou
G. A. McConaghy
and T. J. Hanratty

Department of Chemical Engineering
University of Illinois
Urbana, IL 61801

SCOPE

A paper by McConaghy and Hanratty (1977) presents results of the effect of dilute polymer solutions of Separan AP-30 on measurements of average mass transfer coefficients between a turbulent fluid and a pipe wall for fully developed velocity and concentration fields. They found that the decrease in the mass transfer rate, caused by the addition of polymers, at a given volumetric flow rate, is greater than the percent change in the pressure gradient, and that the use of an analogy between momentum and mass transfer overpredicts

the amount by which the mass transfer rate is decreased.

This paper shows how drag-reducing polymers affect the fluctuations in the mass transfer coefficient. It is based on measurements presented in theses by McConaghy (1974) and Vassiliadou (1983). The motivation for this paper is the testing of ideas that have emerged from recent numerical experiments that simulated turbulent mass transfer at a wall (Campbell and Hanratty, 1983).

CONCLUSIONS AND SIGNIFICANCE

Drag-reducing polymers cause a large decrease in the magnitude of the mass transfer fluctuations, $(\overline{k^2})^{1/2}/\overline{K}$, and change the character of the function describing the fluctuating mass transfer coefficient, $k(t)$. The function does not have the large pulses found for a Newtonian fluid, and is described reasonably well by a Gaussian distribution. Furthermore, the frequency characterizing $k(t)$, made dimensionless with wall parameters, is less than for a Newtonian fluid.

Campbell and Hanratty (1983) have argued that the hydrodynamic property controlling turbulent mass

transfer is the zero frequency value of the dimensionless spectral density function, $W_\beta(0)$, characterizing the normal component of velocity fluctuations in the immediate vicinity of the wall. This quantity is calculated from the measurements of the spectral function of the mass transfer fluctuations that are presented. It is found to decrease with increasing drag-reduction.

The dependence of the time-averaged mass transfer coefficient on $W_\beta(0)$ is found to be the same as predicted in the numerical experiments of Campbell and Hanratty. However $(\overline{k^2})^{1/2}/\overline{K}$ is found to be more strongly dependent on $W_\beta(0)$. This suggests that other hydrodynamic variables than $W_\beta(0)$ need to be considered.

Eleni Vassiliadou is at the Koninklijke Shell Laboratory, Amsterdam, The Netherlands. G. A. McConaghy is at the Amoco Research Center, Naperville, IL.

Introduction

Electrochemical techniques described by McConaghy and Hanratty (1977) were used to study the effect of drag-reducing polymers on the rate of turbulent mass transfer. The test section, which was the cathode of an electrolysis cell, consisted of a length of platinum-plated brass pipe. The electric current, I , is related to the mass transfer rate, N , to the test section by the equation

$$N = I/n_e F, \quad (1)$$

where n_e is the number of electrons involved in the reaction and F is Faraday's constant. A mass transfer coefficient, K , can be defined as follows:

$$K = N/A(C_b - C_w), \quad (2)$$

where A is the electrode area, C_b the bulk concentration of the reacting species, and C_w the concentration at the wall. By operating the cell at a high enough voltage the reaction rate at the cathode surface is very high and $C_w \approx 0$.

Measurements of the time-averaged current to the whole cathode, $\langle I \rangle$, under this polarization condition gives the average mass transfer coefficient from the equation

$$\langle K \rangle = \frac{\langle I \rangle}{n_e A F C_b}. \quad (3)$$

Local time-varying mass transfer coefficients, $K(t)$, can be determined by measuring the current to a small wire embedded flush with the cathode surface and insulated from it. From such measurements the local time-averaged mass transfer coefficient, \bar{K} , and statistical properties of the fluctuating mass transfer coefficient, $k = K - \bar{K}$, can be determined.

Campbell and Hanratty (1983) solved numerically the unaveraged mass balance equations for a randomly varying velocity field for large Schmidt numbers. The result is a randomly varying concentration field from which the time-varying mass transfer coefficient can be calculated. For large Schmidt numbers the concentration boundary layer is thin enough that the velocity field can be represented by the first term in a Taylor series expansion in distance from the wall, y :

$$u = \alpha(x, z, t)y \quad (4)$$

$$w = \gamma(x, z, t)y \quad (5)$$

$$v = \beta(x, z, t)y^2 \quad (6)$$

Campbell and Hanratty argued that the rate of mass transfer to the wall is primarily related to $\beta(z, t)$ and, in particular, to its frequency spectrum, $W_\beta(\omega)$, defined as

$$\bar{\beta}^2 = \frac{1}{2\pi} \int_{-\infty}^{+\infty} W_\beta(\omega) d\omega. \quad (7)$$

The interesting result coming from this work is the suggestion that the most energetic eddies at the wall are not controlling mass transfer. Only low-frequency eddies containing a very small fraction of the turbulent energy are important. From these

computer experiments the following equations were derived for \bar{K} and k^2 :

$$\bar{K} = 0.09 \left[\frac{2 W_\beta(0)}{0.01} \right]^{0.21} Sc^{-0.7} \quad (8)$$

$$\frac{(k^2)^{1/2}}{\bar{K}} = 0.592 [W_\beta(0)]^{0.06} Sc^{-0.06} \quad (9)$$

Here, and in all equations that follow, the variables are made dimensionless using the wall variables, u^* and ν . Campbell (1981) also verified that $W_\beta(0)$ can be evaluated from measurements of $W_k(\omega)$ at high frequency by using the linear theory developed by Sirkar and Hanratty (1970).

$$W_k(\omega) = W_\beta(\omega) \frac{\bar{K}^2 4}{\omega^3 Sc} \quad (10)$$

Equations 8 and 10 represent a complete theory in that they relate the rate of mass transfer to measurable properties of the turbulence close to a wall, since, over the range of frequencies of interest, $W_\beta(\omega)$ is approximately constant and equal to $W_\beta(0)$.

Campbell and Hanratty (1983) also argued that the characteristic frequency of the mass transfer fluctuations can be obtained by assuming $(\partial C/\partial t) \sim (1/Sc)(\partial^2 C/\partial y^2)$ or that $\omega \sim Sc^{-1} \delta^{-2}$, where δ is the thickness of the concentration boundary layer. The thickness δ , which is defined as $\delta \sim K^{-1} Sc^{-1}$, is estimated from Eq. 8. It follows that

$$\omega_c \sim W_\beta(0)^{0.42} Sc^{-0.40} \quad (11)$$

This Schmidt number dependency is in excellent agreement with what has been found by Shaw and Hanratty (1977) for Newtonian fluids. Shaw and Hanratty also found that the spectral function for the mass transfer fluctuations is described by similarity arguments whereby

$$\frac{W_k(\omega)}{k^2 \omega_c^{-1}} = f\left(\frac{\omega}{\omega_c}\right) \quad (12)$$

is a universal function. This argument was found to be supported by spectral measurements for Newtonian fluids over the range of Schmidt numbers 695–16,900. If similarity arguments hold, it follows from Eq. 10 (Shaw and Hanratty, 1977) that

$$\frac{k^2^{1/2}}{\bar{K}} \sim W_\beta^{0.08}(0) Sc^{-0.1}. \quad (13)$$

It is noted that this is different from Eq. 9. This reflects likely errors in the numerical experiments used to produce Eqs. 8 and 9, rather than in the similarity arguments. In any case the difference between Eqs. 9 and 13 is not great.

Equation 8 requires further investigation because the representation of the influence of the velocity field entirely in terms of $W_\beta(0)$ seems an oversimplification. Because law of the wall arguments suggest that dimensionless $W_\beta(0)$ is invariant for a Newtonian fluid, it is not possible to gain further insight by varying the flow rate and pipe diameter. However, it is possible to vary $W_\beta(0)$ by adding drag-reducing polymers. The reduction of $W_\beta(0)$ by this technique is determined by measuring the fre-

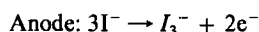
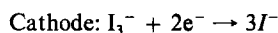
quency spectrum of the mass transfer fluctuations and applying Eq. 10 to the high-frequency part of the spectrum.

The main motivation of this work is to test the accuracy of Eqs. 8, 9, and 11 by using measurements of \bar{K} , \bar{k}^2 , and $W_k(\omega)$ obtained with drag-reducing solutions.

Experimental

The experiments were carried out in a 2.54 cm pipe with a fully developed turbulent flow over a range of Schmidt numbers of 700–1,200. The test fluid was an aqueous solution of iodine, potassium iodide, and a high molecular weight polyacrylamide, Separan AP-30, with concentration of 50, 150, and 325 ppm. The test loop and the experimental techniques are described in papers by Shaw and Hanratty (1977) and by McConaghy and Hanratty (1977).

A schematic diagram of the test system is given in Figure 1. The cathode, which was the test section, consisted of a 6.35 cm long brass pipe plated with platinum. The anode consisted of sections of pipe both upstream (6.35 cm long) and downstream (1.52 m long) of the cathode so as to reduce the ohmic potential drop in the test section. The reactions were as follows:



The current flowing to the whole cathode gives \bar{K} from Eq. 3. The local mass transfer coefficient $K(t)$ was determined by measuring the current to platinum wires located flush with the cathode surface. These were at a dimensionless distance of $x > 3,000$ from the upstream edge of the cathode so as to insure that the concentration boundary layer was fully developed (McConaghy and Hanratty, 1977). An electronic circuit was used to measure and eliminate the mean current from the local electrodes and to amplify the fluctuating component. Details regarding the fabrication of the test section and the measuring techniques are given by Vassiliadou (1983), and McConaghy (1974), and in previously cited papers.

These experiments could not be conducted at too high a Reynolds number because the electric current, and therefore the

Table 1. Physical and Solution Properties for Experimental Runs

Separan AP-30 Conc., ppm	ν , cm ² /s	D , cm ² /s
0	8.18×10^{-3}	1.16×10^{-5}
20	8.60×10^{-3}	0.92×10^{-5}
150	9.17×10^{-3}	0.89×10^{-5}
325	10.66×10^{-3}	0.89×10^{-5}
Composition of the electrolyte solution		
C_{KI} (mol/L): 0.5		
C_{I_2} (mol/L): 1.5×10^{-4} – 2.5×10^{-4}		

voltage drop, in the solution become too high. If the voltage drop along the length of the cathode exceeded the range of applied potential over which the reaction is diffusion-controlled, the electrode could not be polarized. In order to minimize this effect the iodine concentration, and therefore the current, is kept as low as possible. At these low concentrations it was necessary to keep the potassium iodide concentration high enough so that the residual current is small compared to the current associated with the electrode reactions. One way to operate at low iodine concentrations and yet have a measurable signal is to use a larger test electrode. However, there is a limit to this choice because of averaging of the mass transfer fluctuations over the electrode surface (Shaw and Hanratty, 1977). These kinds of considerations lead to the choice of iodine concentrations of 1.5×10^{-4} to 2.5×10^{-4} M, test electrode diameters of 0.254, 0.320, and 0.404 mm, potassium iodide concentrations of 0.5 M, and Reynolds numbers from 27,000 to 43,000.

The electrolyte and polymer solutions were freshly prepared before each experiment, following a standard procedure described by McConaghy (1974). The polymer solutions exhibited a Newtonian shear stress-shear rate relationship because of the low concentration of Separan AP-30. Their kinematic viscosities were measured with a Canon-Fenske viscometer. The diffusion coefficient of the I_3^- ion was determined by a method described by Torini et al. (1978). Typical values are summarized in Table 1. A decrease of D with increasing polymer con-

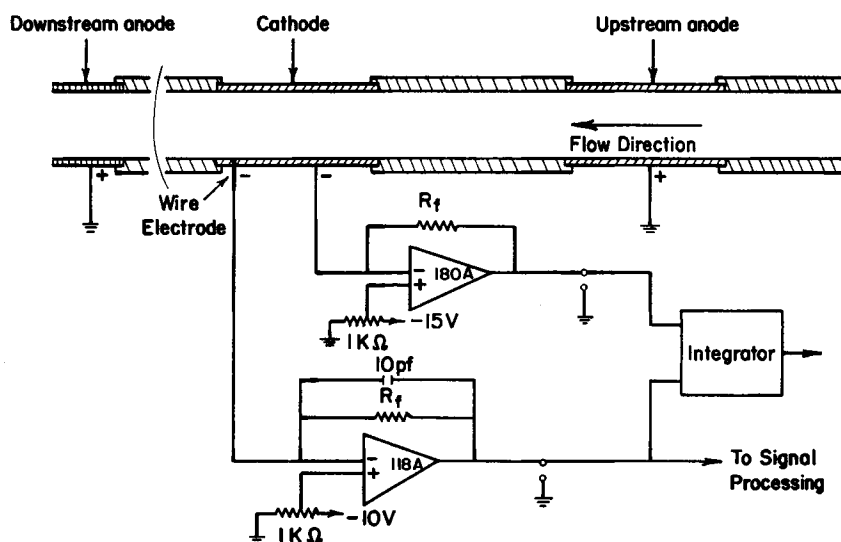


Figure 1. Mass transfer test section and electronic circuit.

centration is noted. The value of $D = 1.16 \times 10^{-5}$ cm²/s, obtained with no polymer, is close to the values of 1.13×10^{-5} reported by Newson and Riddiford (1961) and 1.18×10^{-5} by Shaw (1976) and Chin (1971) for the same system.

The fluctuating component of the current to the test electrodes was sampled at 100 Hz to obtain more than 60,000 points for each experiment. The fluctuating mass transfer coefficient, $k(t)$, defined as

$$K(t) = \bar{K}(t) + k(t) \quad (14)$$

is directly related to the fluctuating current, $i(t)$, by the equation

$$k(t) = \frac{i(t)}{n_e A F C_B} \quad (15)$$

The mean squared value of $k(t)$ is evaluated as

$$\bar{k}^2 = \frac{1}{N} \sum_{i=1}^N k_i^2, \quad (16)$$

where i denotes the i th sample and N the sample size.

The probability density function was calculated with the following relation:

$$P\left(\frac{k}{\bar{K}}\right) = \lim_{\Delta(k/\bar{K}) \rightarrow 0} \frac{1}{\Delta\left(\frac{k}{\bar{K}}\right)} \left[\lim_{T} \frac{T_k}{T} \right] \quad (17)$$

where T is the total number of data points and T_k is the number of data points between k and $k + \Delta k$.

The frequency spectrum of the mass transfer fluctuations is defined by the relation

$$\bar{k}^2 = \frac{1}{2\pi} \int_{-\infty}^{+\infty} W_k(\omega) d\omega \quad (18)$$

The method of Welch (1967) was used to calculate $W_k(\omega)$ by the fast Fourier analysis technique (Bendat and Piersol, 1971). The digitized data were separated into segments and a spectrum estimated from each of these periodograms. An average of 128 periodograms (over 60,000 points) was used to obtain the final spectral function. A digital low-pass filter was used for smoothing the digital data before applying the fast Fourier algorithm (Kaiser and Reed, 1977).

Results

Local average mass transfer coefficients

Values of dimensionless \bar{K} are presented in Figure 2 for the solvent and for solutions of Separan having concentrations of 50, 150, and 325 ppm. This plot clearly shows that the mass transfer coefficient for the drag-reducing solutions decreases with increasing concentration of Separan AP-30. The decrease in dimensional \bar{K} is actually larger than is suggested in Figure 2 since the data are normalized with the friction velocity, which is smaller in drag-reducing solutions at the same Reynolds number.

The decrease in dimensionless \bar{K} shown in Figure 2 is interpreted (according to Eq. 8) as being caused either by changes in

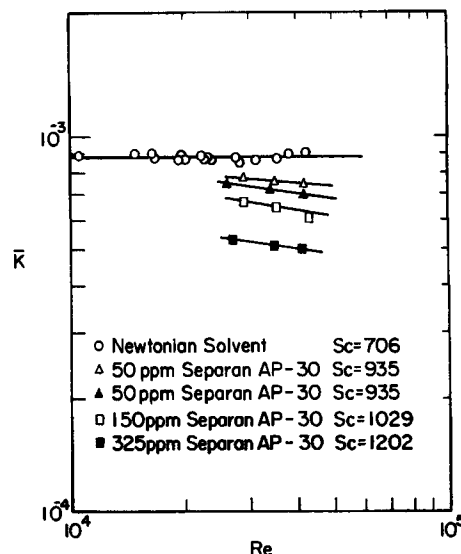


Figure 2. Mass transfer coefficient in solvent and polymer solutions normalized with wall parameters.

the Schmidt number or in $W_\beta(0)$. Figure 3 corrects for the effect of Schmidt number by plotting the factor B_P/B_N defined by McConaghy and Hanratty (1977).

$$\frac{B_P}{B_N} = \frac{[\bar{K} Sc^{0.7}]_P}{[\bar{K} Sc^{0.7}]_N}, \quad (19)$$

where the subscript N signifies the Newtonian solution, and subscript P the polymer solution. The factor B_P/B_N is plotted against the percent drag reduction, defined as

$$\%DR = \left(1 - \frac{\Delta P_P}{\Delta P_N} \right)_Q \times 100, \quad (20)$$

where ΔP_P is the pressure drop for the polymer solution and ΔP_N is the pressure drop for the Newtonian solvent at the same volumetric flow, Q . Figure 3 shows that B_P is less than B_N . This indicates that the presence of the drag-reducing polymer causes changes in the turbulence close to the wall beyond that expected

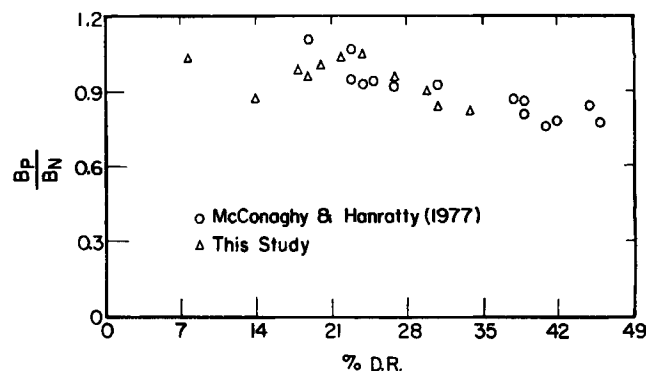


Figure 3. Comparison of mass transfer coefficients for polymer solutions with mass transfer coefficients for Newtonian solutions.

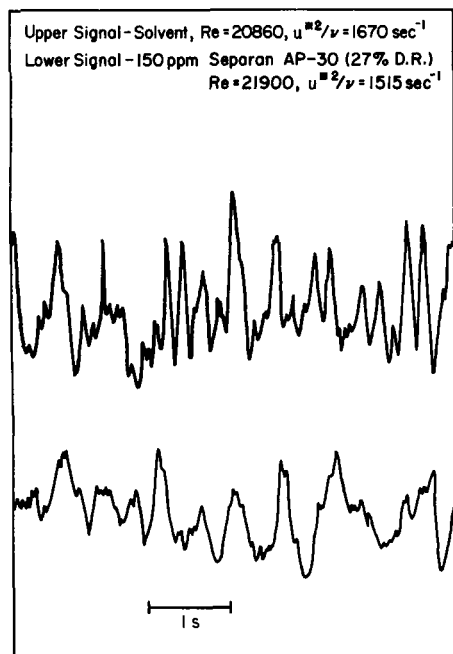


Figure 4. Comparison of mass transfer fluctuations in polymer solution to solvent; 27% drag reduction.

from the decrease in u^* and law of the wall considerations. It is noted that these changes become greater with increased drag-reduction.

Mass transfer fluctuations

A comparison is made in Figure 4 of the measured $k(t)$ for the Newtonian solvent and a polymer solution. Significant differences are noted. The amplitude and frequency of the fluctuations are greater for the Newtonian solvent. In addition, the signal for the drag-reducing solution is smoother and does not show the large positive spikes indicated by the Newtonian signal.

These differences are all evident in quantitative measurements of the fluctuations.

Figure 5 is a plot of $(\overline{k^2})^{1/2} Sc^{0.06}/\overline{K}$ vs. the percent drag reduction. The factor $Sc^{0.06}$ is an attempt to correct for effects of Schmidt number, as suggested by Eq. 9. This plot indicates that the addition of drag-reducing polymer causes $(\overline{k^2})^{1/2}$ to decrease even more than \overline{K} .

The probability density function for 150 ppm polymer solution (27% drag reduction) is compared with that for a Newtonian solvent in Figure 6. The curves shown in these figures are the Gaussian distributions. The Newtonian solvent shows clear-cut non-Gaussian behavior, in that large positive deviations are more likely than large negative deviations. This is evidenced by positive skew factors. Such a behavior is not evident with the polymer solutions for which the skew factors are closer to zero, as can be seen in Figure 6.

Frequency spectra

A comparison of frequency spectra for the solvent and the drag-reducing solution is given in Figure 7. The variables are made dimensionless using wall parameters, and W_k has been normalized with \overline{K}^2 . The drag-reducing solutions are found to have relatively less energy in the high frequencies than the Newtonian solutions. These differences cannot be explained by the small differences in Schmidt number, as can be seen by using the scaling relations developed by Shaw and Hanratty (1977).

These spectra are at low enough frequencies that $W_\beta(\omega)$ is a constant and approximately equal to $W_\beta(0)$. Thus Eq. 10 suggests that $W_k(\omega)/\overline{K}^2$ should vary in n^{-3} at large frequencies, with a proportionality constant equal to $4W_\beta(0)/(2\pi)^3 Sc$. The lines shown in Figure 7, which have slopes of n^{-3} , give reasonable fits to the high-frequency data. Values of $W_\beta(0)$ evaluated from such fits are summarized in Table 2.

It is noted that $W_\beta(0)$ decreases with increasing drag reduction. This indicates that the dimensional value of $W_\beta(0)$ is affected more than would be expected from the decrease in u^* and law of the wall considerations. This is consistent with the finding that B_p/B_N (defined by Eq. 19) is less than unity, and with the prediction by Campbell and Hanratty (1983) (Eq. 8)

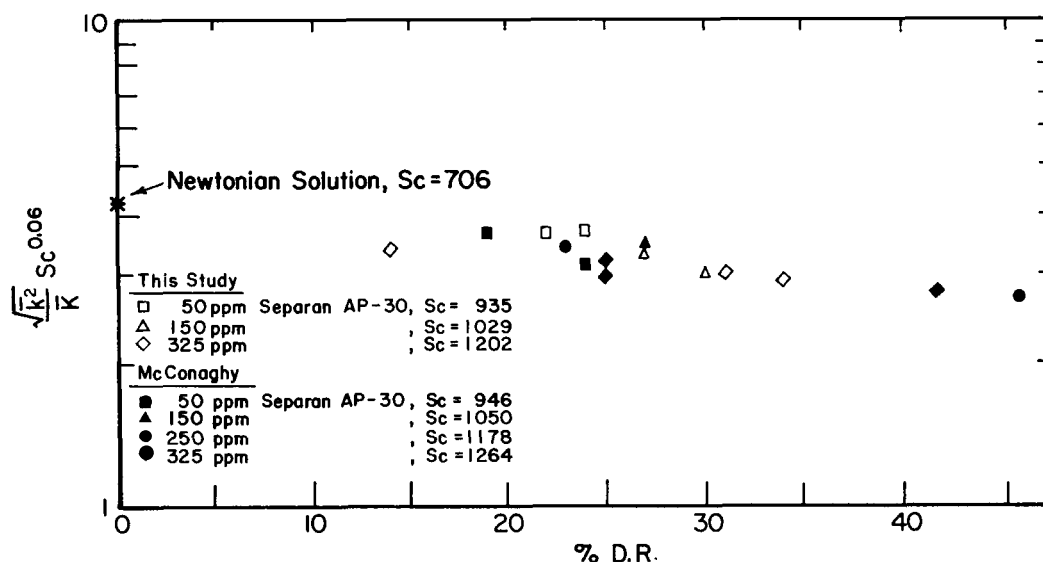


Figure 5. Variation of mass transfer intensity with percent drag reduction.

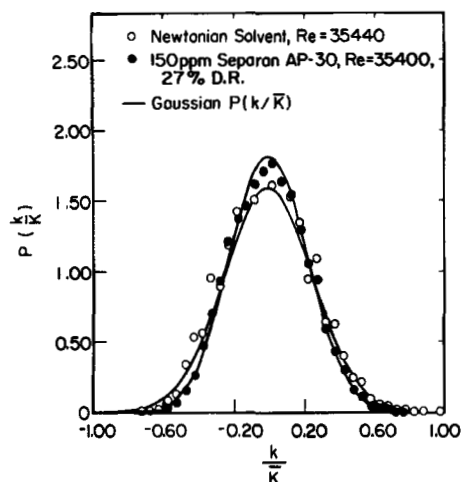


Figure 6. Probability density function for mass transfer fluctuations in polymer solution and solvent.

that decreases in B should be directly related to decreases in $W_\beta(0)$.

The average frequency defined as

$$\langle n \rangle = \frac{1}{k^2} \int_0^\infty n W_k dn \quad (21)$$

is plotted in Figure 8 as $\langle n \rangle Sc^{0.40}$ vs. $W_\beta(0)$. These results show the influence of drag-reducing polymers in reducing the frequency of the mass transfer fluctuations. An equation of the same form as Eq. 11 represents the data reasonably well:

$$\langle n \rangle = 0.232 W_\beta^{0.42}(0) Sc^{-0.40} \quad (22)$$

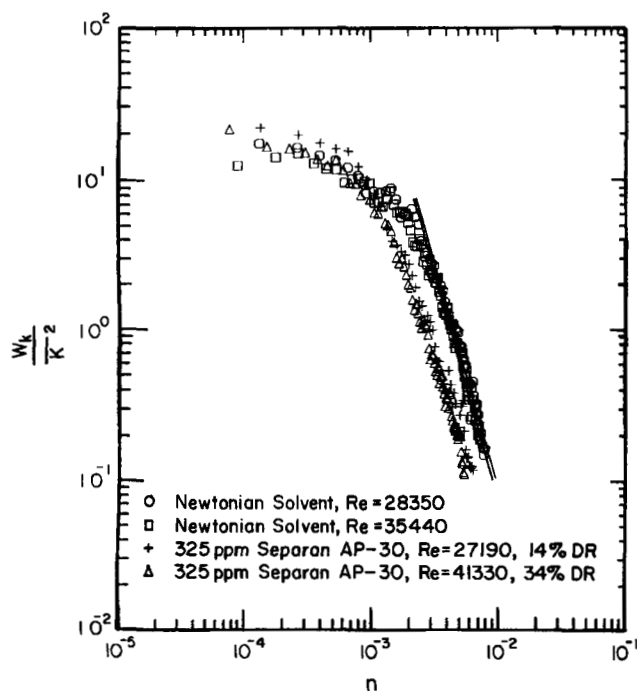


Figure 7. Comparison of mass transfer frequency spectra in polymer solutions with solvent using linear model.

Table 2. Calculated Values for $W_\beta(0)$ Using W_k and Linear Theory

Separan AP-30 Conc. ppm	% Drag Reduction	$W_\beta(0) \times 10^3$
0	24	4.24-4.81
50	22	3.13-3.60
50	22	2.23-2.64
50	8	2.97-3.91
50	18	3.05-3.76
50	20	2.66-3.29
150	27	2.95-3.28
150	30	2.23-2.62
325	14	1.87-2.21
325	31	1.59-1.87
325	34	1.65-2.01

Spectral data for several runs are plotted in Figure 9 in the similarity form suggested by Eqs. 11 and 12. A reasonable correlation is obtained.

Examination of the Campbell Relations

The accuracy of the equation developed by Campbell and Hanratty (1983) for \bar{K} is tested in Figure 10 where $\bar{K} Sc^{0.7}$ is plotted against $W_\beta(0)$. The solid line represents Eq. 8. Good agreement is noted with the exception of two data points for 50 ppm polymer solutions. These data points are actually suspect because they give values of $B_p/B_N > 1$. It is quite possible that errors were made in the determination of u^* .

A comparison of the Campbell and Hanratty equation for the intensity of the mass transfer fluctuations with measurements is given in Figure 11. It is noted that the influence of changes of $W_\beta(0)$ on $(k^2)^{1/2}/\bar{K}$ is much greater than that predicted by Eq. 9.

Discussion

The computer simulation of Campbell and Hanratty greatly simplified the representation of the velocity field in the concentration boundary layer given by Eqs. 4, 5, and 6. By assuming that the concentration and velocity fields are approximately homogeneous in the flow direction, it was argued that $\alpha(x, z, t)$ has little effect and that $\partial\alpha/\partial x \approx 0$. The variation of β in the z

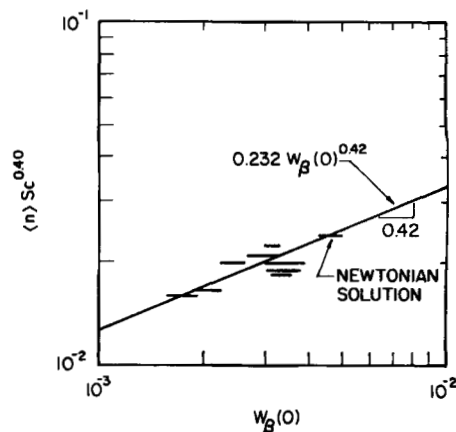


Figure 8. Average frequency of mass transfer fluctuations.

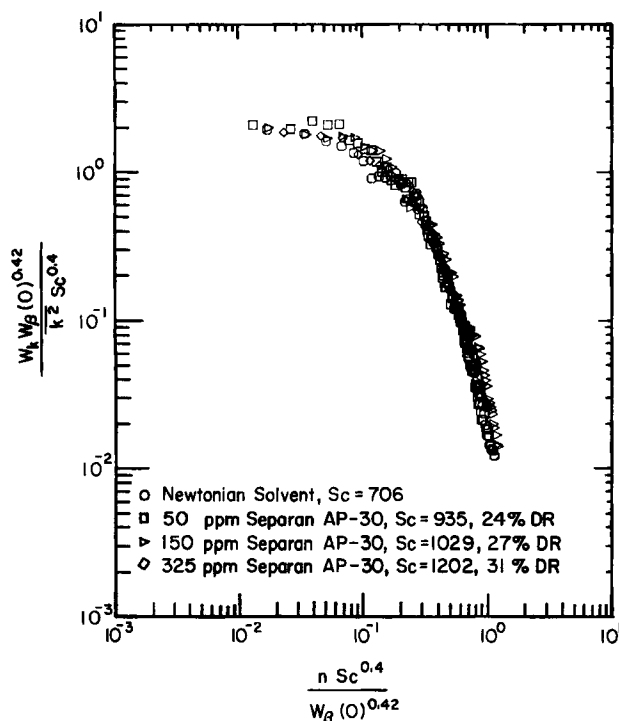


Figure 9. Spectra plotted to show similarity in shape.

direction was represented by a single spatial harmonic so that

$$v = y^2 \beta(t) \cos\left(\frac{2\pi z}{\lambda_z}\right), \quad (23)$$

where λ_z is the scale of the velocity fluctuations in the spanwise direction. The spanwise velocity field is calculated from Eq. 23 using the equation of conservation of mass

$$\frac{\partial \gamma}{\partial z} + 2\beta(t) \cos\left(\frac{2\pi z}{\lambda_z}\right) = 0. \quad (24)$$

Measurements by Campbell and Hanratty (1983) suggest

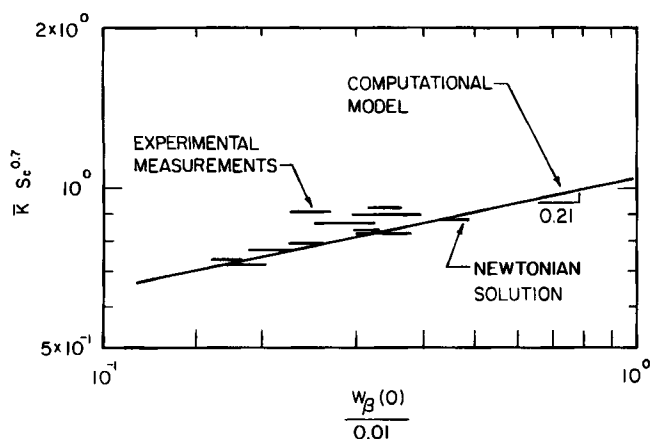


Figure 10. Comparison of mass transfer coefficient predicted with 2-D model to experimental measurements.

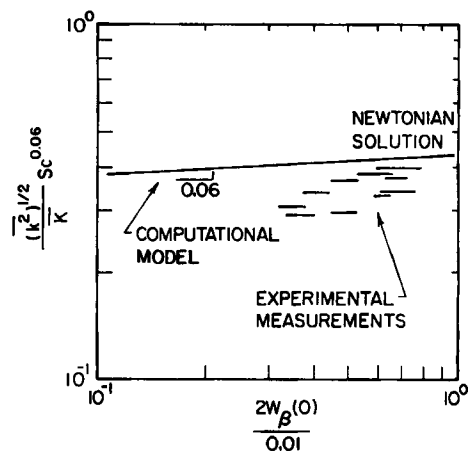


Figure 11. Comparison of relative intensity of mass transfer coefficient predicted with 2-D model to experimental measurement.

that the dimensionless spanwise wavelength is $\lambda_z = 50$ –100 for a Newtonian fluid. In the computer solution, $\beta(t)$ was obtained from laboratory measurements by Campbell (1981) of $(\Delta\gamma/\Delta z)$ for $\Delta z = 4.93$. Good agreement is noted between the laboratory measurements and the values of \bar{K} obtained from this computer simulation, Eq. 9. However, the poor agreement between the values of $(\bar{k}^2)^{1/2}/\bar{K}$ obtained in the laboratory and computer experiments is not completely understood. A number of possibilities exist.

The most obvious possibility is that the wavelength, λ_z , as well as $W_b(0)$, should appear in the equations defining \bar{K} and \bar{k}^2 . Campbell and Hanratty varied λ between 50 and 100 and found little effect. As has been shown by Fortuna and Hanratty (1972), the presence of drag-reducing eddies can cause the dimensionless spanwise scale characterizing the velocity field to be much larger than 100.

Another possibility is that the presence of drag-reducing polymers causes fundamental changes in the low-frequency velocity fluctuations not characterized by $W_b(0)$ and λ . Some support for this explanation is obtained from the finding that the $k(t)$ signal becomes less pulsatile with the addition of drag-reducing polymers.

Acknowledgment

This research was supported by the National Science Foundation under Grant NSF CPE 82-19065 and by the Shell Companies Foundation.

Notation

- A = area of the electrode, cm^2
- B = constant, Eq. 15
- C_B = bulk-averaged concentration of the diffusing species, mol cm^3
- C_w = concentration of the diffusing species at the wall, mol/cm^3
- D = molecular diffusion coefficient, cm^2/s
- d = diameter of the tube, cm
- F = Faraday's constant = 96,500 coul/cq
- I = electric current, coul/s
- i = fluctuating electric current
- K = mass transfer coefficient, cm/s , made dimensionless with u^* (except in Eqs. 2 and 3)
- k = fluctuations in the mass transfer coefficient made dimensionless using u^*

N = mass transfer rate, mol/s
 n = frequency in Hz made dimensionless with u^* and ν
 $\langle n \rangle$ = average frequency, Eq. 21
 n_e = equivalents per mole of reactant in electrolytic reaction, eq/mol
 $P(k/\bar{K})$ = defined in Eq. 17
 ΔP = pressure difference, g/cm² · s
 Re = Reynolds number = $d \cdot U_B / \nu$
 Sc = Schmidt number = ν / D
 t = time made dimensionless with u^* and ν
 U_B = bulk-averaged velocity, cm/s
 u = fluctuating streamwise velocity made dimensionless with u^*
 u^* = friction velocity, cm/s
 v = fluctuating normal velocity made dimensionless with u^*
 W_k = spectral density function for k normalized with ν
 w = fluctuating transverse velocity made dimensionless with u^*
 W_β = spectral density function for β normalized with u^* and ν
 x = coordinate in streamwise direction made dimensionless with u^* and ν
 y = coordinate perpendicular to wall made dimensionless with u^* and ν
 z = coordinate transverse to flow made dimensionless with u^* and ν

Greek letters

α = defined in Eq. 4
 β = defined in Eq. 6
 γ = defined in Eq. 5
 λ_z = wavelength of the spatial scale in the transverse direction made dimensionless with u^* and ν
 ν = kinematic viscosity, cm²/s
 ω = circular frequency made dimensionless with u^* and ν
 ω_c = characteristic frequency of the mass transfer fluctuations

Subscripts

N = Newtonian solution
 P = polymer solution

Symbols

— = time average
 $\langle \rangle$ = spatial average; the average defined as the first moment of the spectral function

Literature Cited

- Bendat, J. S., and A. G. Piersol, *Random Data: Analysis and Measurement Procedures*, Wiley, New York, 300–309 (1971).
 Campbell, J. A., "The Velocity-Concentration Relationship in Turbulent Mass Transfer to a Wall," Ph.D. Thesis, Univ. Illinois, Urbana (1981).
 Campbell, J. A., and T. J. Hanratty, "Mechanisms of Turbulent Mass Transfer at a Solid Boundary," *AIChE J.*, **29**, 221 (1983).
 Chin, D. T., "An Experimental Study of Mass Transfer on a Rotating Spherical Electrode," *J. Electrochem. Soc.*, **118**, 1,764 (1971).
 Fortuna, G., and T. J. Hanratty, "The influence of Drag-Reducing Polymers on Turbulence in the Viscous Sublayer," *J. Fluid Mech.*, **53**, 575 (1972).
 Kaiser, J. F. and W. A. Reed, "Data Smoothing Using L-P Digital Filters," *Rev. Sci. Instrum.*, **48**, 1,447 (1977).
 McConaghy, G. A., "The Effect of Drag-Reducing Polymers on Turbulent Mass Transfer," Ph.D. Thesis, Univ. Illinois, Urbana, (1974).
 McConaghy, G. A., and T. J. Hanratty, "Influence of Drag-Reducing Polymers on Turbulent Mass Transfer to a Pipe Wall," *AIChE J.*, **23**, 493 (1977).
 Newson, J. D., and A. C. Riddiford, "Limiting Currents for the Reduction of the Tri-Iodine Ion at a Rotating Platinum Ring Cathode," *J. Electrochem. Soc.*, **108**, 695 (1961).
 Shaw, D. A., "Mechanism of Turbulent Mass Transfer to a Pipe Wall at High Schmidt Number," Ph.D. Thesis, Univ. Illinois, Urbana (1976).
 Shaw, D. A., and T. J. Hanratty, "Influence of Schmidt Number on the Fluctuations of Turbulent Mass Transfer to a Wall," *AIChE J.*, **23**, 160 (1977).
 Sirkar, K. K., and T. J. Hanratty, "Relation of Turbulent Mass Transfer at High Schmidt Numbers to the Velocity Field," *J. Fluid Mech.*, **44**, 589 (1970).
 Tonini, R. D., M. R. Remorino, and F. M. Brea, "Determination of Diffusion Coefficients with a Pipe Wall Electrode," *Electr. Acta*, **23**, 699 (1978).
 Vassiliadou, E., "Effect of Drag-Reducing Polymers on Turbulent Mass Transfer," M.Sc. Thesis, Univ. Illinois, Urbana (1983).
 Welch, P. D., "The Use of Fast Fourier Transforms for the Estimation of Power Spectra: A Method Based on Time-Averaging over Short, Modified Periodograms," *IEEE Trans. Audio Electroacoust.*, **15**, 70 (1967).

Manuscript received Dec. 7, 1984, and revision received June 12, 1985.